

Resonant tunneling magneto resistance in coupled quantum wells

Christian Ertler* and Jaroslav Fabian†

Institute for Theoretical Physics, University of Regensburg, D-93040 Regensburg, Germany

A three barrier resonant tunneling structure in which the two quantum wells are formed by a dilute magnetic semiconductor material (ZnMnSe) with a giant Zeeman splitting of the conduction band is theoretically investigated. Self-consistent numerical simulations of the structure predict giant magnetocurrent in the resonant bias regime as well as significant current spin polarization for a considerable range of applied biases.

Semiconductor spintronics offers new functionalities to the existing electronics technology by combining charge and spin properties of the current carriers [1]. The goal of spintronic devices is to modulate charge current by changing the electron spin. In magnetic tunnel junctions, for example, magnetic electrodes are sandwiched around a nonmagnetic tunnel barrier, yielding large magnetocurrents (relative current magnitudes for parallel and antiparallel orientations of the electrodes' magnetizations) [1]. In other spintronic devices, e.g., magnetic resonant tunneling diodes [2, 3, 4, 5, 6, 7, 8], the transmission at a given voltage can depend strongly on the spin orientation of the electrons at the Fermi level. Such diodes have been used as spin filters or spin detectors.

Here we propose to use magnetic resonant tunneling diodes comprising coupled magnetic quantum wells and three nonmagnetic barriers, as spintronic devices offering large magnetocurrents. Such devices combine the geometry of magnetic tunnel junctions with magnetic resonant tunneling diodes. Corresponding three-barrier nonmagnetic structures have been experimentally studied [9, 10, 11, 12]. The magnetic three barrier structure allows to establish parallel and antiparallel magnetization configurations and to observe magnetocurrent. The origin of the magnetization here is not essential. The quantum wells can be either dilute magnetic semiconductors [13], which have giant g-factors at temperatures up to 100 K, or they could be ferromagnetic quantum wells [14, 15, 16] in which the splitting is given by the exchange field. Performing realistic selfconsistent calculations of the I-V characteristics we indeed predict large magnetocurrents (say, 10000% for a moderate spin splitting of 10 meV) at resonant voltages. These large values appear because of the suppression of the resonant tunneling due to the energy mismatch for the resonant levels of the coupled wells in the antiparallel configuration. Although the predicted effect is rather robust, we provide hints on how to further tune the heterostructure parameters to maximize the magnetocurrent.

We investigate a three barrier semiconductor het-

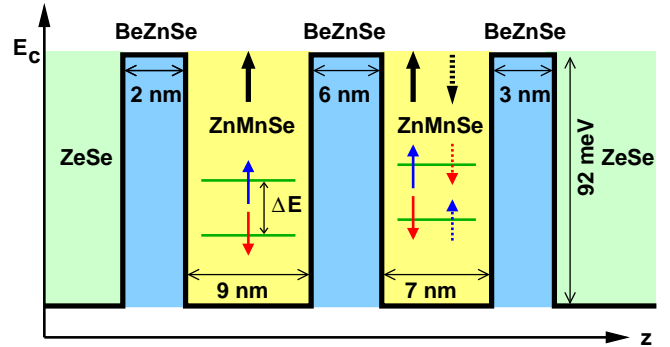


FIG. 1: (Color online) Schematic conduction band profile of an all II-IV semiconductor three barrier heterostructure. The quasibound states in the quantum wells are Zeeman-split by an external magnetic field.

erostructure based on a Zn(Be,Mn)Se material system. The conduction band profile at zero bias is schematically shown in Fig. 1. The barriers are formed by Be-doped ZnSe, whereas the quantum wells (QWs) are made of the dilute magnetic semiconductor (DMS) material ZnMnSe. Such a system is an extension of a two barrier structure already experimentally investigated in Ref. [2]. Following a previous theoretical work [17] on two-barriers structures, we assume the barrier height to be 92 meV, which is about 23% of the band gap difference between ZnSe and ZnBeSe. In DMSs an external magnetic field B causes a giant Zeeman energy splitting ΔE into spin up and spin down electron states, which can be expressed by the modified Brillouin function B_s [8]:

$$\Delta E = x_{\text{eff}} N_0 \alpha s B_s (g_{Mn} s \mu_B B / k_B T_{\text{eff}}). \quad (1)$$

Here, x_{eff} is the effective concentration of Mn ions, $N_0 \alpha = 0.26$ eV is the $sp-d$ exchange constant for conduction electrons, $s = 5/2$ is the Mn spin, $g_{Mn} = 2.00$ is the Mn g-factor, μ_B labels the Bohr magneton, k_B denotes Boltzmanns constant, and T_{eff} is an effective temperature. At low temperatures (all simulations are performed at a lattice temperature of $T = 4.2$ K), Mn concentrations of about 8%, and practical magnetic fields of 1-2 T, the giant electron g-factor in the DMS leads to an energy splitting of the conduction band of about 10 meV [2]. The whole structure is considered to be sandwiched between two leads consisting of n -doped ZnSe ($n = 10^{18}$

*email: christian.ertler@physik.uni-regensburg.de

†email: jaroslav.fabian@physik.uni-regensburg.de

cm^{-3}) of 10 nm width. Similar to experiments [2], we include 5 nm thick undoped ZnSe buffer layers between the leads and the active structure, which causes an upward band bending at zero bias.

Following the classic treatments of (two barriers) resonant tunneling diodes [18, 19, 20], we assume coherent transport throughout the whole active region. This is a reasonable assumption also for our three barriers magnetic diode, since signatures of coherence, namely the splitting of the well states into bonding and antibonding states, have been observed experimentally in such structures [9]. We calculate the spin dependent current flow by numerically solving the conduction band effective mass Schrödinger equation taking into account the spin dependent potential energy,

$$U_i(z) - e\phi(z) + \sigma\Delta E(z). \quad (2)$$

Here, U_i is the intrinsic conduction band profile, e is the elementary charge and $\sigma = \pm 1/2$, (\uparrow, \downarrow) labels the spin quantum number. The electrostatic potential ϕ is obtained from the Poisson equation, which is solved together with the Schrödinger equation in a self-consistent way. The current density of electrons with spin σ is calculated by

$$j_\sigma = \frac{e}{(2\pi)^3} \int d^3k v_z T_\sigma(E_l, E_t) [f(E) - f(E + eV_a)], \quad (3)$$

where E_l and E_t are, respectively, the longitudinal and transverse component of the electron total energy E , V_a denotes the applied voltage, $T_\sigma(E_l, E_t)$ is the electron transmission function, v_z labels the longitudinal component of the electron group velocity, and $f(E) = 1/[1 + \exp(E - E_f)/k_B T]$ is the Fermi function with the Fermi energy E_f . Assuming parabolic bands and using the same effective mass $m_*/m_0 = 0.145$ (with m_0 denoting the free electron mass) for all layers of the heterostructure, the transmission function only depends on the longitudinal energy, $T(E_l, E_t) = T(E_l)$. This allows to reduce Eq. (3) to the Tsu-Esaki formula [21]. The current spin polarization is then determined by $P_j = (j_\uparrow - j_\downarrow)/(j_\uparrow + j_\downarrow)$.

We assume that the magnetization of the first QW is fixed, whereas the second is 'soft', which means that it is sensitive to local changes of an external magnetic field. Hence, a magnetocurrent MC can be defined as the relative difference of the current I for parallel (P) and antiparallel (AP) alignment of the magnetization of the two quantum wells, $MC = (I_P - I_{AP})/I_{AP}$. The proposed structure aims in producing very high MCs based on the following idea of operation. High resonant tunneling throughout the whole structure is possible if the middle barrier is thin enough and if two quasi-bound states of same spin of the adjacent QWs are aligned energetically. Such resonant condition for the lowest energy states in the case of P magnetization is illustrated in the inset of

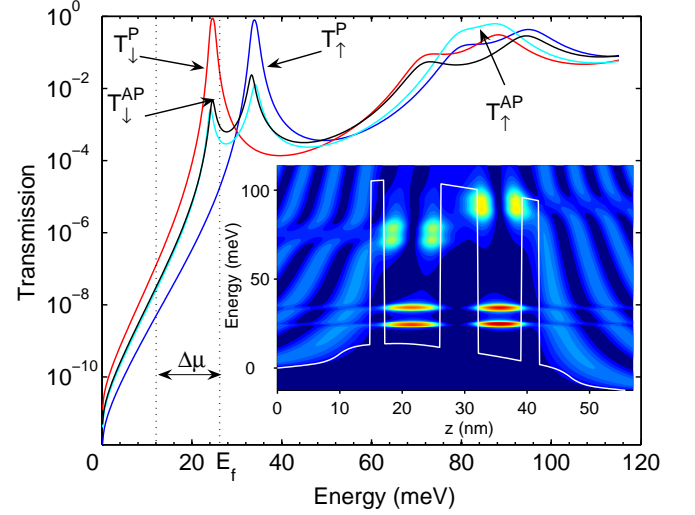


FIG. 2: (Color online) The spin resolved energy-dependent transmission function at $T = 4.2$ K for parallel (P) and antiparallel (AP) magnetization in the case of a given Zeeman splitting of $\Delta E = 10$ meV and a resonant applied voltage of $V_a = 13$ meV. The inset shows a contour plot of the local density of states versus energy and growth direction z at resonance ($V_a = 13$ mV) for parallel magnetization and $\Delta E = 10$ meV. The solid line indicates the self-consistent conduction band profile. The higher quasibound states (at about 80 and 90 meV) are not in resonance.

Fig. 2. The inset shows the local density of states of the conduction electrons and clearly demonstrates the Zeeman splitting of the quasibound states into spin up and spin down states. Here, the orientation of the magnetic field is assumed such that the spin down (up) energy levels are shifted downwards (upwards) in energy. Due to the interaction of the two QWs the resonant energy levels are further split into bonding and antibonding states. The splitting is observable in the local density of states if it is greater than the natural energy broadening of the quasibound state. For our structure the middle barrier is too thick to resolve this additional splitting in the plot of the local density of states. The inset of Fig. 2 also shows higher quasibound states at about 80 and 90 meV, which are however not in resonance.

In the case of P magnetization the spin up and down quasibound states are equally Zeeman shifted in both QWs, whereas for AP alignment they are shifted energetically in opposite directions. Assuming QWs of the same width, i.e., with the same quasi-bound energy spectrum, there are hence at equilibrium open resonant conduction channels for the P alignment, whereas the transmission is blocked for the AP configuration. However, when a small finite voltage is applied to the structure the resonant channels of the P magnetization are 'destroyed', since the energy levels of the second QW are shifted more deeply to lower energies than those of the first QW by the

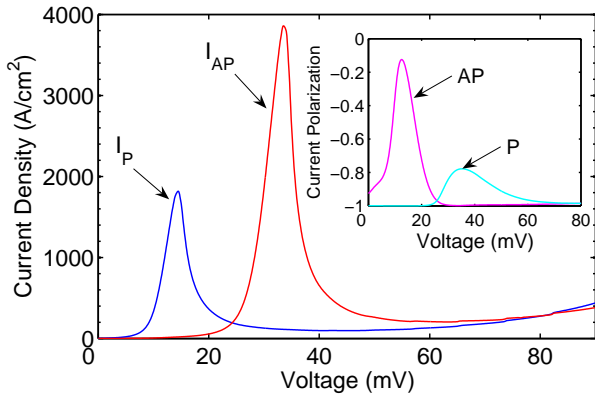


FIG. 3: (Color online) Current-Voltage characteristics of the structure for parallel (P) and antiparallel (AP) magnetization at the temperature $T = 4.2$ K and the Zeeman splitting of $\Delta E = 10$ meV. The inset displays the current polarization as a function of the applied voltage.

applied bias. To overcome this shortcoming, we propose to use asymmetric QWs. Here, we take the second QW to be thinner than the first one. This gives rise to a higher ground state energy in the second QW and the resonant condition is therefore adjusted at a finite voltage, leading to high currents.

In order to maximize the MC we pursue the following strategy for determining the different layer widths. At low temperatures the current is given, in good approximation, by the quadrature of the transmission function over the energy window $\Delta\mu = [E_f - eV_a, E_f]$. To obtain high currents for the P alignment, the layer widths should be chosen such, that the resonant tunneling condition, $T(E) \approx 1$, is fulfilled at a finite voltage for energies belonging to the interval $\Delta\mu$. On the other hand, for the AP configuration the transmission function should be made as small as possible in the energy window $\Delta\mu$. To meet both demands at the same time, we use a relatively thin middle barrier, which effectively controls the coupling of the QWs. Figure 2 shows the spin-resolved transmission function versus energy for the resonant voltage $V_a = 13$ mV. The double peak structure of the transmission function for the AP configuration corresponds to the lowest quasibound state in both QWs, which have in that case different energies leading to two 'half-resonances'. The transmission for the AP alignment can be strongly hampered by choosing thick QWs. The variation of the thickness of the first and third barrier barely influences the MC, since the transmission is then either reduced or increased for both P and AP magnetization. By changing the buffer layer thicknesses one can tune the amount of band bending and hence, the relative position of the quasi-bound energies to the Fermi level. The dimensions of the structure finally used in our numerical calculations are indicated in Fig. 1.

The obtained current-voltage characteristics for P and

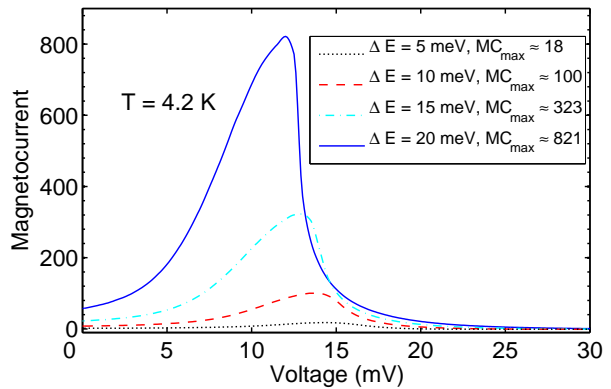


FIG. 4: (Color online) Magnetocurrent (MC) as a function of applied voltage for different Zeeman splittings ΔE .

AP magnetization and a fixed Zeeman splitting of $\Delta E = 10$ meV are displayed in Fig. 3. In the case of P magnetization, the lowest quasibound energy levels of the adjacent QWs are already aligned at a small voltage of about 13 mV, whereas for the AP configuration a much higher voltage is necessary to obtain resonant tunneling. The current spin polarization is plotted in the inset of Fig. 3. Since the spin down state has a lower energy than the spin up state, the current for P magnetization is almost all spin down polarized at low voltages. For higher voltages also spin up states contribute to the current thereby diminishing the polarization. In the case of AP magnetization, spin up current can flow at low voltages due to the lowest spin up state in the second QW. By increasing the voltage this state gets off resonance, which leads again to significant spin down polarization. The obtained MCs for different Zeeman energy splittings are shown in Fig 4. The transmission for AP magnetization is strongly reduced by increasing the energy splitting ΔE . Hence, the current for AP magnetization becomes very small at the peak voltage of the P configuration and our simulations reveal very high MCs up to 800 for reasonable spin splitting. Simulations performed at a higher temperature $T = 100$ K show that the MC is reduced to about 25% of its value at $T = 4.2$ K. Although the temperature effect is quite large, the MC remains significant.

To summarize, we have numerically investigated an all semiconductor three barrier resonant tunneling structure, comprising two quantum wells made of a magnetic material. Our simulations predict very high magnetocurrents demonstrating the device potential of the proposed structure. Further investigations of an *in-plane* (perpendicular to the growth direction of the heterostructure) resistance of the two coupled magnetic QWs promise to reveal interesting effects, since resistance resonances for such a current-in-plane configuration have already been demonstrated for nonmagnetic structures [22].

This work has been supported by the Deutsche

-
- [1] I. Žutić, J. Fabian, and S. Das Sarma, *Rev. Mod. Phys.* **76**, 323 (2004).
- [2] A. Slobodskyy, C. Gould, T. Slobodskyy, C. R. Becker, G. Schmidt, and L. W. Molenkamp, *Phys. Rev. Lett.* **90**, 246601 (2003).
- [3] T. Hayashi, M. Tanaka, and A. Asamitsu, *J. Appl. Phys.* **87**, 4673 (2000).
- [4] P. Bruno and J. Wunderlich, *J. Appl. Phys.* **84**, 978 (1998).
- [5] I. Vurgaftman and J. R. Meyer, *Phys. Rev. B* **67**, 125209 (2003).
- [6] A. Voskoboynikov, S. S. Lin, C. P. Lee, and O. Tretyak, *J. Appl. Phys.* **87**, 387 (2000).
- [7] T. Gruber, M. Keim, R. Fiederling, G. Reuscher, W. Ossau, G. Schmidt, L. W. Molenkamp, and A. Waag, *Appl. Phys. Lett.* **78**, 1101 (2001).
- [8] N. N. Beletskii, G. P. Berman, and S. A. Borysenko, *Phys. Rev. B* **71**, 125325 (2005).
- [9] Y. Zohata, T. Nozu, and M. Obara, *Phys. Rev. B* **39**, 1375 (1989).
- [10] A. Palevski, F. Beltram, F. Capasso, L. Pfeiffer, and K. W. West, *Phys. Rev. Lett.* **65**, 1929 (1990).
- [11] L. D. Macks, S. A. Brown, R. G. Clark, R. P. Starrett, M. A. Reed, M. R. Deshpande, C. J. L. Fernando, and W. R. Frensley, *Phys. Rev. B* **54**, 4857 (1996).
- [12] A. Newaz, W. Song, and E. E. Mendez, *Phys. Rev. B* **71**, 195303 (2005).
- [13] J. K. Furdyna, *J. Appl. Phys.* **64**, R29 (1988).
- [14] A. Oiwa, R. Moriya, Y. Kashimura, and H. Munekata, *J. Magn. Magn. Mater.* **272** (2004).
- [15] J. Furdyna, T. Wojtowicz, X. Liu, K. M. Yu, W. Walukiewicz, I. Vurgaftman, and J. R. Meyer, *J. Phys.: Condens. Matter* **16**, S5499 (2004).
- [16] T. Dietl, *Semicond. Sci. Technol.* **17**, 377 (2002).
- [17] P. Havu, N. Tuomisto, R. Väänänen, M. J. Puska, and R. M. Nieminen, *Phys. Rev. B* **71**, 235301 (2005).
- [18] M. O. Vassell, J. Lee, and H. F. Lockwood, *J. Appl. Phys.* **54**, 5206 (1983).
- [19] M. Cahay, M. McLennan, S. Datta, and M. S. Lundstrom, *Appl. Phys. Lett.* **50**, 612 (1987).
- [20] W. Pötz, *J. Appl. Phys.* **66**, 2458 (1989).
- [21] R. Tsu and L. Esaki, *Appl. Phys. Lett.* **22**, 562 (1973).
- [22] Y. Berk, A. Kamenev, A. Palevski, L. N. Pfeiffer, and K. W. West, *Phys. Rev. B* **50**, 15420 (1994).